Title	Surface textures and friction control in microforming(Main Article)
Author(s)	Castagne, Sylvie; Taureza, Muhammad; Song, Xu
Citation	Castagne, S., Taureza, M., & Song, X. (2014). Surface textures and friction control in microforming. Advanced materials research, 966-967, 111-119.
Date	2014
URL	http://hdl.handle.net/10220/24162
Rights	© 2014 Trans Tech Publications. This is the author created version of a work that has been peer reviewed and accepted for publication by Advanced Materials Research, Trans Tech Publications. It incorporates referee's comments but changes resulting from the publishing process, such as copyediting, structural formatting, may not be reflected in this document. The published version is available at: [Article DOI: http://dx.doi.org/10.4028/www.scientific.net/AMR.966-967.111].

SURFACE TEXTURES AND FRICTION CONTROL IN MICROFORMING

SYLVIE CASTAGNE[1] *AND MUHAMMAD TAUREZA*[1] *AND XU SONG*[2]
[1] *School of Mechanical and Aerospace Engineering, Nanyang Technological University, Singapore*
[2] *Forming Technology Group, Singapore Institute of Manufacturing Technology, Singapore*

Abstract

Tribological surface textures are considered in this paper as a non-traditional friction control solution for microforming. Textured pads fabrication techniques are first evaluated and load-controlled micro-embossing is chosen as the optimal method to produce repeatable textured patterns on metallic pads. Using tribometer experiments and finite element simulations of dry contact between untextured and textured surfaces for pressure levels representative of microforming conditions, it is shown that there are competing mechanisms creating a sinusoidal-like friction reduction behavior when surface textures are present. Ultimately, it is concluded that a proper design of surface textures and loading conditions can be used for friction reduction in microforming.

Keywords**:** Friction, testing, microforming, texture

1 INTRODUCTION

In metal forming, lubrication and the quality of the surface finish of the tooling are carefully designed in order to control friction. Generally, high friction in metal forming should be avoided as it results in excessive tool wear, high process load requirements and damaged parts. However, studies have shown that due to the reduced size in microforming, there is a shift in friction behavior, called the friction size-effect [1-3]. Because of this shift, the knowledge of friction in conventional metal forming, such as the typical friction coefficient for certain material pairs and performance of lubricants, is not directly applicable to microforming. In particular, past investigations by Engel have shown that friction increases with miniaturization in microforming [2]. These findings have been confirmed by Taureza et al. who characterized various lubricants using a microforming T-Shape test [4] and concluded that there is a microforming-specific phenomenon leading to the loss of lubricant effectiveness [5].

Tribological surface texturing is proposed in this paper to respond to the increase in friction in microforming. Surface textures in microforming should adhere to the following requirements: be fabricated on the dies, lower friction appreciably, do not pose significant negative effect (for example to the part surface finish), and be retained after repeated cycles to reduce cost of die maintenance.

Extensive results on various metals and ceramics have been published on friction control using surface textures, or tribological surface texturing, for both lubricated [6] and unlubricated [7] conditions. The application of surface texturing in microforming has been studied by Brinksmeier et al. [8] through experimentation with the strip drawing test and

Eriksen et al. with the strip reduction test [9]. Through the strip drawing test, it was observed that lowest friction is observed not using the smoothest or roughest sample but rather that there is an optimum finish. Moreover, this investigation on microforming is limited to those based on sheet metal forming and the application to bulk metal forming with higher typical contact pressure has been limited to its implication to tool life [10, 11]. In general, the studies on optimized surface for microforming have only been associated with the effect of surface roughness (not highly defined textures).

Previous studies have mostly focused on two geometries: parallel grooves and pores. The results showed that the friction reduction can be attributed to some parameters: texture area density [12], texture size [13] and texture geometry [14]. Pores or holes [12, 15-17] have been identified as beneficial textures with the trend of reducing friction as pore size to contact area ratio increases (larger pore) [15]. However, introducing too many pores (higher surface area fraction) can impair the texture beneficial effect [13, 16, 17] by increasing the friction and/or promoting wear. Uehara et al. [12] proposes that too much pores results in increased contact pressure (because of less load bearing area) which further increases friction.

Wear particles entrapment has been proposed as the friction-reduction mechanism for unlubricated contact [18]. However, results suggest that the friction-reduction has initiated at very small sliding distance at which wear particles are unlikely to have been generated [7, 18]. Wear particles are removed from surface as wear sheets which are generated only through creation of sub-surface cracks. Through repeated sliding, these micro-cracks coalesce to form larger cracks. The wear particles (in the form of sheets) get delaminated from the surface only after the crack reaches a critical size. In lubricated contact, the friction-reduction has been attributed to lubricant entrapment to enable the lubricant to remain on the surface [12] and to enhanced hydrodynamic lubrication [16] for boundary lubrication and full film lubrication [19], respectively. However, experiments have suggested that friction-reduction can also be reached in water-immersed sliding setup [6]. These findings suggest that the wear particles and lubricant entrapments are not the only friction-reducing mechanisms attributed to surface textures. Therefore, further research is needed to better understand the underlying mechanisms of friction reduction in the case of textured surfaces sliding contact.

The scope in this the study is to investigate the effect of surface texture on the friction behaviour by tribometer experiments and finite element simulations throughout the range of contact pressures relevant to micro metal forming. Various methods to create surface textures are also presented.

2 MANUFACTURING SURFACE TEXTURES

In the context of micro metal forming, tribological surface textures are highly defined surface features introduced on the surface of the tool with the objective of friction control. The current investigation considers surface textures with texture size of approximately 100 µm. These textures are commonly fabricated using processes such as laser machining, lithography, abrasive jet machining or patterning using hard tool. In this study, three fabrication methods were evaluated: laser micro-machining, micro-drilling and micro-embossing. Alicona InfiniteFocus form measurement instrument was used for textures imaging and analysis.

2.1 Laser micro-machining

Surface textures were fabricated on hardened SLD Magic tool steel surface using a 533 nm wavelength Q-switch Nd:YAG nano-second laser. The target aspect ratio for the pore texture was set as depth to diameter ratio of 0.1 as it was shown by Amanov et al. that aspect ratio closer to 0.1 produces the lowest friction [20].

Using long pulse laser for surface texturing, the laser fluence and number of pulses irradiated from the laser source determines the geometry of the resulting pore. However, the disadvantage faced in using laser for surface texturing is that the results were not repeatable as presented in Figure 1. Moreover, long pulse laser creates very significant bulge on the rim of the pore in Figure 1 (a) as the heat energy from the long pulses resulted in material melting and solidification rather than ablation.

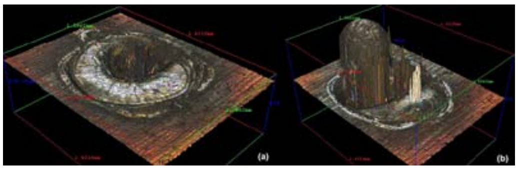

Figure 1: Non-repeatability of long pulse laser for surface texturing between (a) and (b)

2.2 Micro-drilling

The second method evaluated to produce pore textures was micro-drilling. Disadvantages of this method included bulge surrounding the pores and poor control of the side surface of the pore texture as presented in Figure 2.

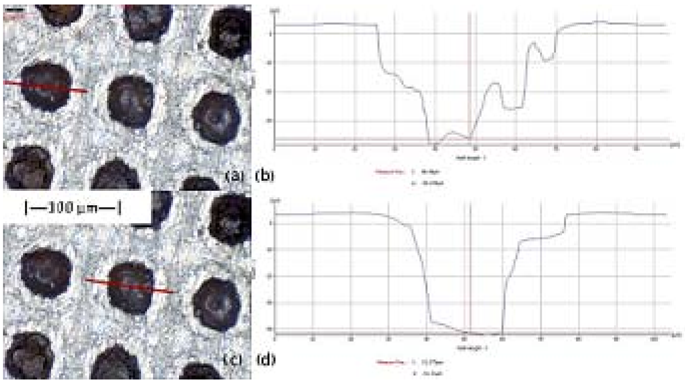

Figure 2: Inconsistent walls from micro-drilling, (a) and (c) micrographs of pore structure indicating selected holes, (b) and (d) corresponding hole line profiles

2.3 Micro-embossing

The micro-embossing technique was selected for the fabrication of the textured surfaces. The principle of this technique is to create a male textured pad which produces the corresponding female surface textures. In this study, the textures were produced through load-controlled embossing using the Schmidt ServoPress 420 with load-control resolution of 100 N [21]. Load-control mode is selected for embossing due to the limited rigidity of the C-frame configuration of the press and low displacement-control resolution of 10 µm provided by the system. Two pads were fabricated with full array of round- and square pores (Figure 3 and Figure 4), respectively. Tool steel AISI D2 was used as the material for the embossing tool. The male textured pad was created using wire electro-discharge machining.

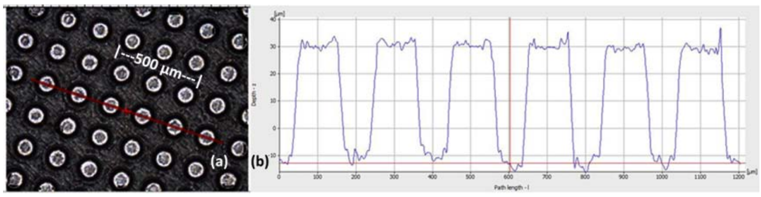

Figure 3. (a) Optical image of male textured pad for round pore surface texture and (b) corresponding line profile

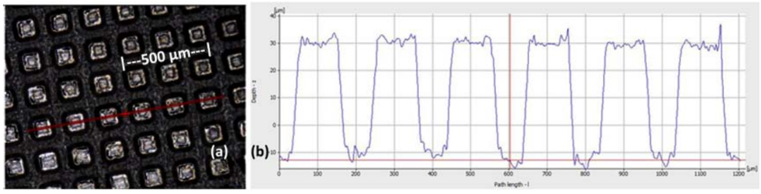

Figure 4. (a) Optical image of male textured pad for squared pore surface texture and (b) corresponding line profile

Two materials were initially chosen for the analysis: ETP copper and AISI 316L stainless steel. Aspect ratio between 0.10 and 0.15 was selected for all the textures produced.

Inter-pore creases were observed during the post texturing examination for copper material. These creases significantly roughen the surface of the textured material. Ultimately, these creases were not observed on textured stainless steel 316L material (Figure 5).

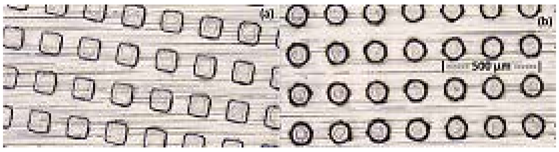

Figure 5: Resulting textures with (a) square and (b) round pore pad on stainless steel

3 TRIBOMETER EXPERIMENTS

Pin on plate test was conducted using CETR UMT3 tribometer to evaluate the friction reduction behavior of textured surfaces. Stainless steel 316L plates, untextured and with round pore texture, were selected for the tribometer experiment.

The pin was made of AISI D2 tool steel with a circular tip of 1 mm diameter. Fillet around the circular tip was necessary to avoid ploughing of the plate material by the sharp edge and therefore the effective contact diameter was reduced to 0.7 mm. A small contact area was required in order to reach large contact pressures representative of the microforming conditions. The circular tip was finished by fine grinding to create surface finish of approximately Ra 0.9 – 1.0 µm.

The experimental results of the untextured pin on flat experiment are presented in Figure 6. Tribometer test is generally conducted for repetitive sliding at low contact pressure (up to tens of MPa) and its use for high contact pressure such as in the current study (up to 600 MPa) presents unavoidable experimental artifacts which require correction of experimental data. In Figure 6, there is a significant increase of the friction coefficient between tests at 400 and 450 MPa. This was attributed to the rotational flexure of the tribometer suspension.

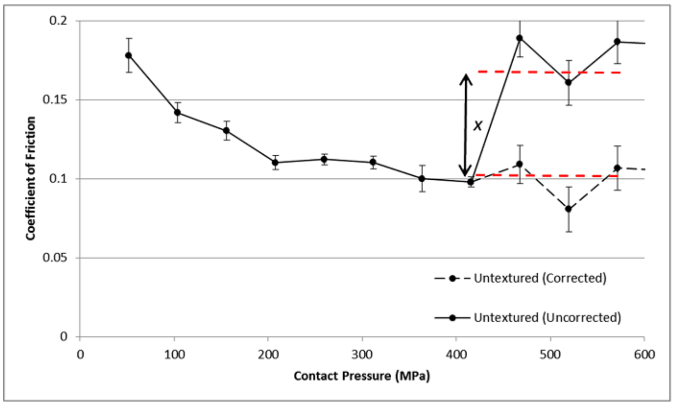

Figure 6: Friction coefficient for untextured pin on plate experiment

In the tribometer test, the pin is connected to the load cell through a suspension to create a smooth contact transition and safeguard the load cell from sudden compression at the start of contact. Although this suspension is optimized to be used for up to 100 kg loading, the suspension was not able to sustain its lateral rigidity. Therefore, at pressure above 400 MPa, the suspension started to flex and the contact between the pin and plate was no longer circular. Consequently, the pin started to plough into the softer plate due to the much reduced effective contact area. This ploughing effect was responsible for the significant increase in the coefficient of friction.

The corrected friction coefficient values were derived by subtracting the coefficient of friction above 450 MPa by the gap between the average coefficient of friction for the immediate three data points higher and lower than 425 MPa and this correction is shown in Figure 6.

Similar experiment on textured surface was conducted and the experimental results (uncorrected and corrected) are presented in Figure 7.

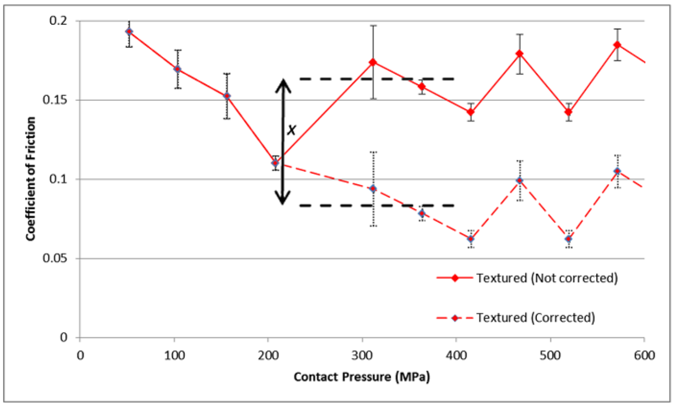

Figure 7: Friction coefficient for textured pin on plate experiment

The friction reduction throughout the range of pressures examined can be quantified by calculating the percentage of friction reduction (%Δμ, Eq. 1 and Figure 8). However, experimental results were not able to provide clear distinction on the limit of texture effectiveness due to variability in the results as presented in Figure 8. As such, a trend line for Figure 8 (with correlation factor of $R^2 > 0.95$) is presented for the material pair in the experiment.

$$\%\Delta\mu = \frac{(\mu_{untex.} - \mu_{tex.})}{\mu_{untex.}} \tag{1}$$

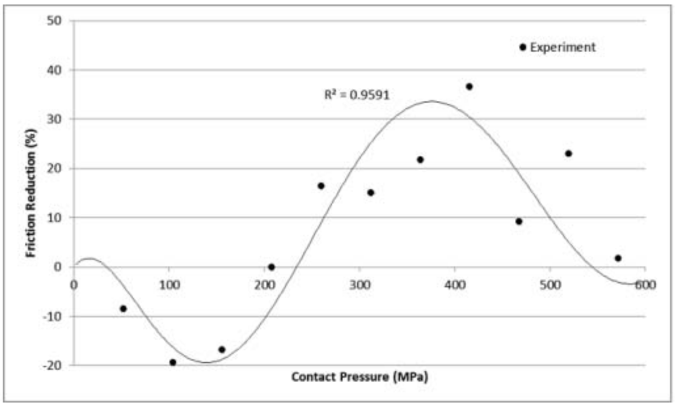

Figure 8: Friction reduction from the addition of surface texture (experiment)

Using the surface texture, a sinusoidal-like behaviour is observed and two distinct regions are highlighted. There is a region with positive effect from surface texture (positive friction reduction, 230 – 550 MPa) and another segment with negative effect from surface texture (negative friction reduction, 50 – 220 MPa). It is important to note that the positive friction reduction is observed only above 230 MPa and that the results at contact pressure above 200 MPa were subjected to data correction (Figure 7). This sinusoidal-like trend is studied using finite element simulation in section 4.

4 PIN ON PLATE SIMULATION

Using Abaqus finite element software, the simulation inputs the material model, pressure-dependent friction coefficient for the flat surface and texture geometry in order to produce a pressure-dependent friction relationship for each given surface texture. The acquired pressure friction relationship can further be used directly in metal forming process simulation in order to simulate the process with surface textures introduced without introducing the texture geometry in the simulation to reduce computational cost. The schematic of the simulation is presented in Figure 9.

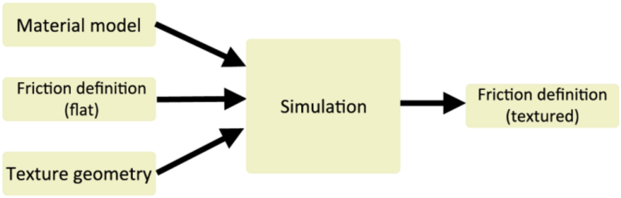

Figure 9: Simulation scheme (input and output)

A round pore texture with a texture density of approximately 20% was modeled as the deformable body with material properties corresponding to stainless steel 316L. On the counter surface, the much harder tool steel is defined as rigid solid with smooth surface.

To conduct the simulation, the textured mesh is pinned at the bottom and the contact pressure is produced by moving the rigid body into the deformable solid. Simultaneously, the textured tool is given a sliding movement parallel to the deformable solid surface with a gradient of ploughing movement of 4%. The simulation was repeated with different displacement values of the rigid body into the deformable solid to provide prediction of friction behavior at various contact pressures. The ratio between the reaction forces along the sliding axis and normal axis was recorded throughout the range of contact pressures to obtain a pressure dependent friction relationship resulting from the simulated texture (Figure 9).

The simulation assumed periodicity of the textured and smooth surface ensuring that the discrete rigid body is in contact with the same number of textures at any time during the simulation. As a control, a similar simulation was also performed using smooth surfaces for both the stainless steel and the tool steel pin.

Comparison between simulation and corrected experimental results for the untextured and textured tool steel pin on stainless steel plate are presented in Figure 10 and Figure 11. The simulation is able to capture the trend from the experiment especially for the untextured setup. Results show that at high contact pressure, there is significant deformation on the softer textured surface which may result in non-performance of the textured surface at high contact pressure as the textures get damaged.

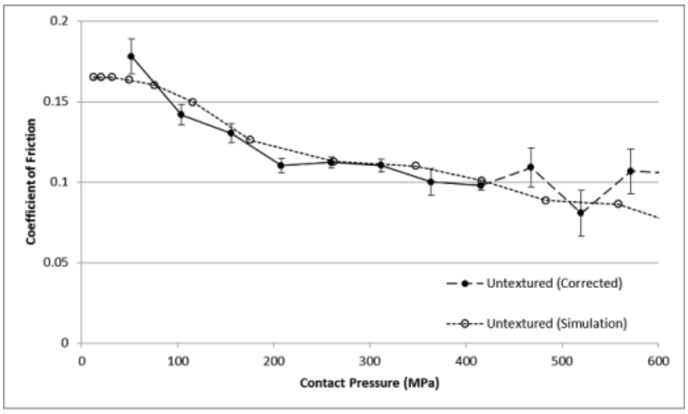

Figure 10: Friction coefficient for pin on plate simulation (untextured)

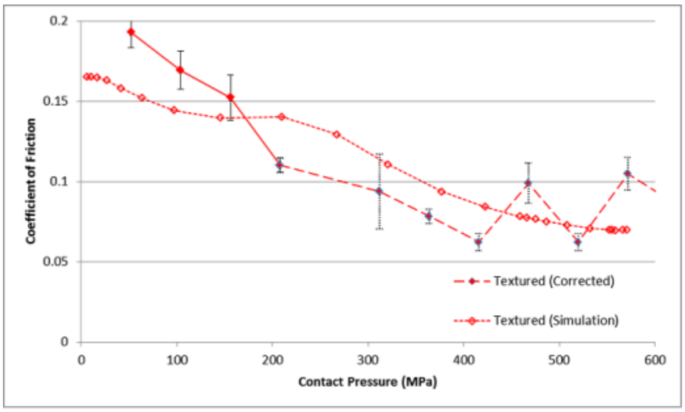

Figure 11: Friction coefficient for pin on plate simulation (textured)

The percentage of friction reduction from the simulation is presented in Figure 12. From the trend line (with correlation factor of R2 > 0.97) drawn in Figure 12, it is observed that the positive effect of surface texture is visible between 30-130 MPa and above 330 MPa. As the simulation does not include defects such as possible bulge on the rim of the individual pores, Figure 12 is therefore representative of cases where the texture does not present any defects. In reality, an observation of the textured stainless steel pad revealed that there is a small amount of bulging between up to 5 μm in height on the rim of the texture. Although this number is small in comparison to the size of the texture, defects such as bulging have been seen to modify the friction behavior [20].

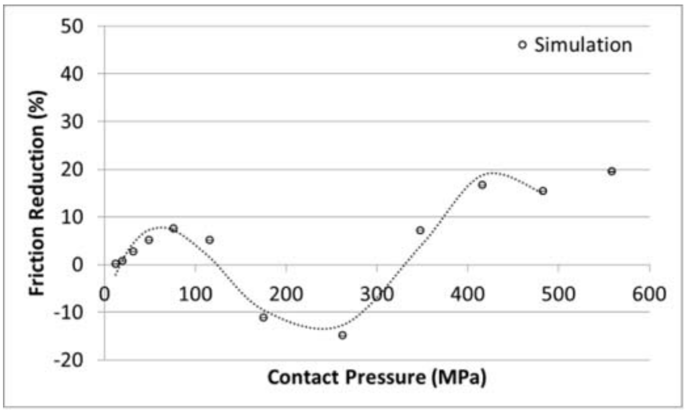

Figure 12: Friction reduction from the addition of surface texture (simulation)

Ultimately, although the range of effective pressure for surface texture from the simulation is not matching exactly the experimental results, the simulation results in general are able to capture the sinusoidal-like behavior observed experimentally. Using the simulation, it was revealed that there is competition between the positive and negative effects of surface textures. The surface textures create smaller friction bearing area in comparison to untextured surface, which results in lower sustainable friction during the contact. However, the surface texture creates irregularity of contact geometry which results in higher rate of material build up at the sliding front.

Observing the simulation results, the friction reduction is positive at low pressure (<130 MPa), this is associated with the saturation of friction stress. At this region, the smaller contact surface in the textured pad limits the maximum sustainable friction. However, as pressure increases, this positive effect is overpowered by the negative effect of deformation of the textured pad (Figure 11) which creates material build up at the deformation front and hinder subsequent sliding. In short, throughout the contact pressure, there is competing physical effect of maximum sustainable friction and material build up at the sliding front (Figure 11). The stronger of the two effects then determines whether or not the texture produces positive effect at a particular contact pressure.

Meanwhile, the discrepancy between experiment and simulation is associated with the defects around the rim of the texture. These defects are irregular in shape and hence the simulation of their behavior is not straightforward. Through the experiment and simulation, it was concluded that the control and characterization of surface defects during texturing are of high interest for research and the mechanism of the defect formation and its influence to friction is considered for future work.

5 SUMMARY AND CONCLUSIONS

Load-controlled micro embossing was selected to create textured metallic surfaces in this study as the technique allows better control and repeatability of the textured produced.

Simulation and experiments were then presented to examine the usefulness of surface texturing as friction control in microforming in dry contact configuration. The simulation results suggest that there are two competing mechanisms when textures are introduced on the tool surface: reducing friction due to the reduced actual contact area, and increasing friction due to material entrapment by the textures.

Those results confirm that by proper design of the surface textures and control of the loading conditions, it will be possible to design tooling surface textures to lower overall friction in microforming.

The simulation of representative textured surface can also be used to define a pressure dependant friction coefficient relationship which can be incorporated directly in microforming process simulation without the need to model the detailed textured surfaces.

6 ACKNOWLEGMENT

This work was undertaken as part of and was funded by the SIMTech Collaborative Research Project (CRP) U11-F- 015SU on Development and study of metal forming system(s) for micro components and features. Funding support through the Nanyang Technological University Research Student Scholarship is also acknowledged.

7 REFERENCES

[1] M. Geiger, *et al.*, "Microforming," *CIRP Annals - Manufacturing Technology,* vol. 50, pp. 445-462, 2001.

[2] U. Engel, "Tribology in Microforming," *Wear,* vol. 260, pp. 265-273, 2006.

[3] F. Vollertsen and Z. Hu, "Tribological size effect in sheet metal forming measured by a strip drawing test," *CIRP Annals*, vol. 55, pp. 291-294, 2006.

[4] M. Taureza, *et al.*, "The influence of die geometry and workpiece mechanical properties in T-Shape friction test," *Journal of Materials Processing Technology,* vol. 212, pp. 2413-2423, 2012.

[5] M. Taureza, *et al.*, "On the influence of workpiece material on friction in microforming and lubricant effectiveness," *Journal of Materials Processing Technology*, vol. In press, 2013.

[6] S. Schreck and K. H. Zum Gahr, "Laser-assisted structuring of ceramic and steel surfaces for improving tribological properties," *Applied surface science,* vol. 247, pp. 616-622, 2005.

[7] A. Borghi, *et al.*, "Tribological effects of surface texturing on nitriding steel for high-performance engine applications," *Wear,* vol. 265, pp. 1046-1051, 2008.

[8] E. Brinksmeier, *et al.*, "Tribological behavior of micro structured surfaces for micro forming tools," *International Journal of Machine Tools and Manufacture,* vol. 50, pp. 425-430, 2010.

[9] R. S. Eriksen, *et al.*, "Manufacture of functional surfaces through combined application of tool manufacturing processes and Robot Assisted Polishing," *CIRP Annals - Manufacturing Technology,* vol. 61, pp. 563-566, 2012.

[10] K. Wagner, *et al.*, "Tool life enhancement in cold forging by locally optimized surfaces," *Journal of Materials Processing Technology,* vol. 201, pp. 2-8, 2008.

[11] M. Geiger, *et al.*, "Excimer Laser Micro Texturing of Cold Forging Tool Surfaces - Influence on Tool Life," *CIRP Annals - Manufacturing Technology,* vol. 51, pp. 231-234, 2002.

[12] Y. Uehara, *et al.*, "Tribological properties of dimpled silicon nitride under oil lubrication," *Journal of the European Ceramic Society,* vol. 24, pp. 369-373, 2004.

[13] M. Wakuda, *et al.*, "Effect of surface texturing on friction reduction between ceramic and steel materials under lubricated sliding contact," *Wear,* vol. 254, pp. 356-363, 2003.

[14] M. Suh, *et al.*, "Effect of geometrical parameters in micro-grooved crosshatch pattern under lubricated sliding friction," *Tribology International,* vol. 43, pp. 1508-1517, 2010.

[15] M. Wakuda, *et al.*, "Effect of surface texturing on friction reduction between ceramic and steel materials lubricated sliding contact," *Wear*, vol. 254, 2003.

[16] X. Wang, *et al.*, "The effect of laser texturing of SiC surface on the critical load for the transition of water lubrication mode from hydrodynamic to mixed," *Tribology International,* vol. 34, pp. 703-711, 2001.

[17] A. Kovalchenko, *et al.*, "The effect of laser surface texturing on transitions in lubrication regimes during unidirectional sliding contact," *Tribology International,* vol. 38, pp. 219-225, 2005.

[18] N. P. Suh, *et al.*, "Control of friction," *Wear*, vol. 175, pp. 151-158, 1994.

[19] W. R. D. Wilson, "Friction and lubrication in bulk metal-forming processes," *Journal of Applied Metalworking,* vol. 1, pp. 7-19, 1978.

[20] A. Amanov, *et al.*, "The influence of bulges produced by laser surface texturing on the sliding friction and wear behavior," *Tribology International,* vol. 60, pp. 216-223, 2013.

[21] X. Song, *et al.*, "Development of low cost deformation-based micro surface texturing system for friction reduction," presented at the ICOMM 2014, Singapore, 2014.